ISSN 2616-5791 Vol.5, Issue 5: 29-40, DOI: 10.25236/AJMHS.2024.050505

Mechanical analysis of metatarsal bone load in patients with varus foot based on finite element method

Wang Kun[1,a,*], Yan Chaowei[1,b], Han Pengfei[1,c]

[1]College of Mechanical Engineering, Inner Mongolia University of Technology, Hohhot, China
[a]2256833546@qq.com, [b]1539634793@qq.com, [c]Hanpf522@hotmail.com
[*]Corresponding author

Abstract: *Currently, it remains unclear about the mechanical effects of different weights and foot varus angles on metatarsal lesions in patients with strephenopodia in the clinical rehabilitation process.In this study,a coupling model related to the lower extremities was established.Besides,some patients with different weight loads and different foot varus angles were included in this study.The effects of some pathological parameters (such as the foot varus angles of 0°,10°,15°,and 20°,as well as the weight loads of 0.5,1,and 2 times the body weight) on the local bone load of feet were analyzed by statics and dynamics numerical simulation methods.These scientific endeavors were made to accurately analyze the point force within the foot bone area under different working conditions.Moreover,the mechanical effects of different foot varus angles and weight loads on five metatarsal bones and lateral tarsometatarsal joints were further revealed through the comparative analysis of the affected foot and the healthy foot.These results indicated that after the foot varus angle increased,a significant difference in the metatarsal load between healthy and affected feet was observed in the fourth and third metatarsal bones,especially the third metatarsal bone.The lateral fifth metatarsal bone was the main weight-bearing component in the affected foot,and hence this part was prone to stress fractures.These findings provided scientific mechanical reference for clinical orthopedic surgeons to implement precise treatment of strephenopodia.*

Keywords: *Stroke; Strephenopodia; Finite element analysis; Biomechanics; Metatarsal stress*

1. Introduction

Strephenopodia is a complex structural pathological condition in clinical practice[1].Compared with healthy individuals,patients with strephenopodia present with abnormalities in the force line joining the Achilles tendon and the heel,asymmetry in the contact area between the medial and lateral forefeet[2].In severe cases,strephenopodia may induce fractures of the lateral bones of feet and falling risks[3].Some scholars from different countries have conducted many explorations into strephenopodia.However,most existing studies are performed through gait experiments based on ankle-foot orthoses (AFOs).There are few attempts to reveal the load patterns of the metatarsal load points in patients with strephenopodia using numerical simulation methods.Furthermore,the mechanical principle also remains to be clarified.

Some scholars have investigated the stress changes in ankle bones after foot strike under different weight loads and foot strike angles (FSAs).When there is an included angle between the calcaneus and the ground,the stress on the metatarsal bone and plantar fascia may increase,thus causing injury to the metatarsal bone and plantar fascia[4].When the FSA of the anterior sole of the foot was larger than 15°,obvious stress concentration would appear in each metatarsal bone under 0.5 times the body weight,which could also induce stress fractures[5].These two studies are involved in the risk of local metatarsal injury in healthy feet; However,the mechanical effect on the affected foot under this working condition was not taken into consideration.The stress in talipes equinovarus (TEV) was mainly concentrated around the ankle joint,and metatarsal fractures had slight impacts on the stress change in the tarsal bone region[6].In their study,a control group was established to analyze the metatarsal stress in patients with TEV and healthy individuals; however,the metatarsal point force at different varus angles was not elucidated.Under a high pressure load,obesity may increase the load on feet for a long term,which would cause injury to soft tissues and bones[7].They reported on the mechanical effects of different weight load parameters on the plantar soft tissue surface force and metatarsal points; however,the metatarsal mechanics under different FSAs were not revealed.During the push-off phase in the stance phase,the stress at the calcaneal tubercle increases,which changes the biomechanical environment of the foot,thus

ISSN 2616-5791 Vol.5, Issue 5: 29-40, DOI: 10.25236/AJMHS.2024.050505

leading to plantar fasciitis and calcaneal pain[8].Although the plantar soft tissue surface force and calcaneal mechanics during the push-off phase were explored in their study,the mechanical effects on the metatarsal bone were not corroborated.

In this study,the finite element numerical simulation method was employed to delve into the local bone stress patterns of feet under some pathological parameters,including the foot varus angles of 0°,10°,15°,and 20°,as well as the weight loads of 0.5,1,and 2 times the body weight.Besides,some healthy individuals were included in the control group.Moreover,the stress patterns of metatarsal points in soft tissues of the affected foot under different varus angles were accurately analyzed,in an attempt to explore the mechanical effects of different body weights on the metatarsal bones of the affected foot.Furthermore,the dynamic data were acquired to reveal the mechanical characteristics of metatarsal points in patients with strephenopodia under different foot strike time points.These findings are expected to provide scientific mechanical reference for clinical orthopedic surgeons to implement the digital and precise treatment for metatarsal lesions in patients with strephenopodia.

2. Materials and Methods

2.1. Construction of the Finite Element Analysis Coupling Model

Mimics software was used to reconstruct the geometric model,as shown in Figure 1.Then,the initial model was imported into Geomagic Studio for data processing.Subsequently,an error analysis was carried out with the calcaneus as an example,as shown in Figure 2.Strephenopodia at the ankle joint was the focus of this study.Given the large range of motion at the ankle joint,the foot bones were fused with articular cartilages in order to improve calculation efficiency.A total of 22 pieces of articular cartilages were generated by using the functions of protrusion stretching and equidistant curved surface between the joints of foot bones[9].Eventually,the tibia,distal fibula,tibiotalar articular cartilage,fibulotalar articular cartilage,and foot bone were preserved.Soft tissues and bones were subjected to Boolean operations.According to a previous study[10],the medial side of the model was rotated at a certain angle to simulate strephenopodia.A support plate (250 mm×150 mm×20 mm) was created to simulate the ground.The final finite element model is shown in Figure 3.

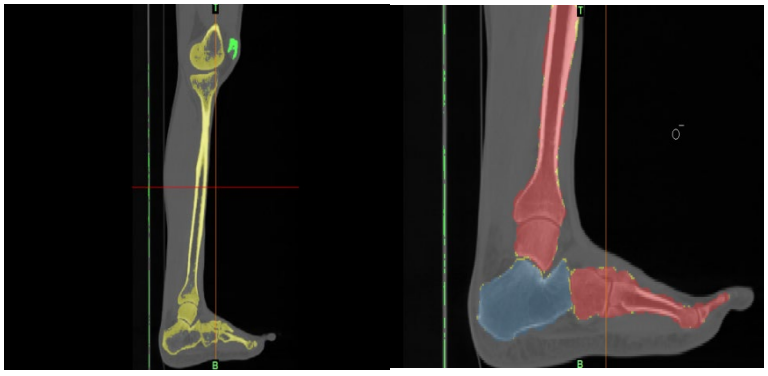

Figure 1: Region growth and bone segmentation.

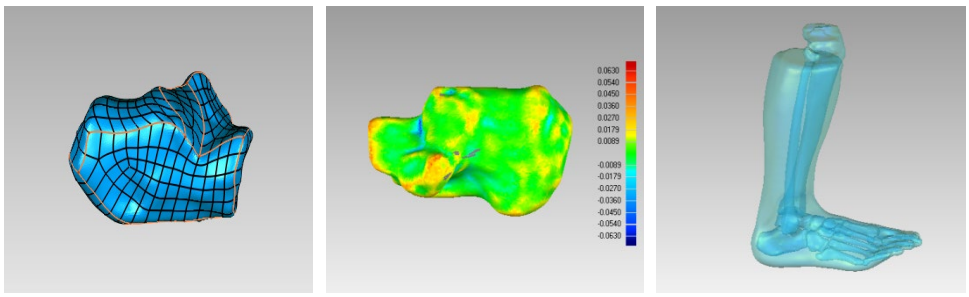

a *b* *c*

Figure 2: Reverse modeling of soft tissues and bone models.a) Curved surface construction.b) Calcaneal precision analysis.c) Ankle-foot coupling model

ISSN 2616-5791 Vol.5, Issue 5: 29-40, DOI: 10.25236/AJMHS.2024.050505

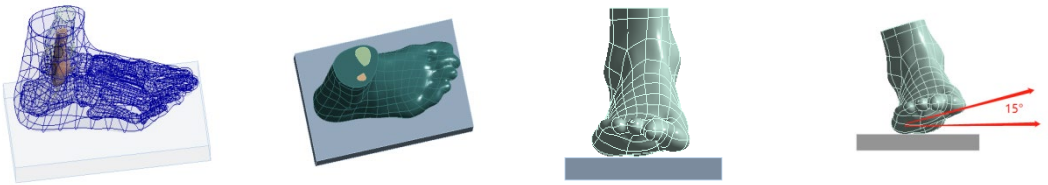

Figure 3: Finite element model of the healthy foot and the simulated affected foot.

2.2. Material Properties and Mesh Generation

A three-dimensional (3D) foot model was imported into ANSYS for tetrahedral mesh generation.According to some previous studies[11,12],the size of the soft tissue was set to 4 mm,the size of the tibia and fibula was set to 3 mm,the high-precision geometric detail of the articular cartilage was set to 0.5 mm,and the contact area between soft tissues and the ground was set to 2 mm.The regular floor was in the shape of a hexahedron,with a size of 10 mm,and included a total of 430,227 cells and 668540 nodes.From the perspective of material properties,the material was assumed to be an isotropic linear elastomer[13].According to the ligament establishment method of He Xiaoyu et al.[6],the Springs element in finite element software was utilized to simulate the main ligament of ankle joints.The starting and ending points at both ends of the ligament were connected to the adjacent skeletal surfaces.Ligament distribution was constructed according to previous studies,such as Atlas of Human Anatomy,and 3Dbody Anatomy (ShangHai QiaoMedia Information Technology Co.,Ltd.,China).These ligaments were mainly composed of the anterior talofibular ligament,calcaneofibular ligament,tibiocalcaneal ligament,and others.The mechanical properties of materials are listed in Tables 1 and 2[14,15,16,17].

Table 1: Parameters of various structural materials in the finite element model

Model	Young's modulus (MPa)	Poisson's ratio	Density (Kg/m^3)
Skeleton	7300	0.3	1500
Articular cartilage	1	0.4	937
Soft tissue	0.45	0.49	937
Ground	17000	0.1	/

Table 2: Ligament material parameters

Ligament	Stiffness (N/mm)
Anterior talofibular ligament	141.8
Anterior inferior tibiofibular syndesmosis ligament (proximal and distal)	90,78
Anterior tibiotalar ligament	122.6
Calcaneofibular ligament	126.6
Posterior talofibular ligament (2)	82
Inferior tibiofibular syndesmosis interosseous ligament	234
Posterior inferior tibiofibular syndesmosis ligament (proximal and distal)	90,101
Posterior tibiotalar ligament (4)	60
Tibionavicular ligament	39.1
Tibiocalcaneal ligament (2)	63

ISSN 2616-5791 Vol.5, Issue 5: 29-40, DOI: 10.25236/AJMHS.2024.050505

2.3. Linear Elastic Constitutive Model

It is necessary to explore the properties of materials for removing practical problems.A constitutive equation is an equation that describes the relationship between two physical quantities (such as stress and stress change rate,as well as strain and strain rate)[18].There is a linear relationship between stress and strain in the microstructure,which can form a linear elastic constitutive model.Under small stress conditions,stress on human bones,muscles,and ligaments may exhibit a linear relationship. Therefore, linear elastic materials with isotropy can be used to replace nonlinear viscoelastic materials for analysis.This will not only improve the calculation efficiency,but also ensure the accuracy of the results.In general,the relationship between the stress and strain can be expressed as Hooke's Law,namely:

$$\sigma = E \cdot \varepsilon \tag{1}$$

where, E represents the elastic modulus; ε represents the strain; σ represents the stress.

In the 3D space, the constitutive relation of linear elasticity can be expressed as:

$$\sigma_{ij} = E_{ijkl}\varepsilon_{kl} \tag{2}$$

where, σij represents the component of the stress tensor; εkl represents the component of the strain; Eijkl represents the component of the elastic modulus.

2.4. Setup of Contact and Boundary Condition

The enhanced Lagrange algorithm was applied to the contact setup.The flexible body was set as the contact surfaces; while the rigid body was set as the target surfaces.Based on this principle,bones,cartilage,and soft tissues were set as the binding contact in this study.The soft tissue was set as the contact surface,and the hard bone was set as the target surface.The friction contact was set between articular cartilages,namely tibiotalar joint and fibulotalar joint,with a friction coefficient of 0.002[16] to simulate the sliding state of human joints.Besides,the friction contact was set between the plantar soft tissue and the ground,with a friction coefficient of 0.6[7].

2.5. Statics Setup

The soft tissue was fully fixed and restrained to the upper surface of the tibiofibula.The body mass load was determined to be 330 N based on the body mass on a single foot,and the force was concentrated to act vertically upward on the central lower surface of the bottom plate.The force on the Achilles tendon was equal to 75% of the body mass load on one foot[19].This value was determined to be approximately 247 N,which was applied to the node at the calcaneal tubercle.The freedom of the floor in the X and Y axes was limited,and the floor was only allowed to move in the Z axis,as shown in Figure 4 (a).

2.6. Dynamics Setup

The bearing capacity of the metatarsal bone is the main difference between patients with strephenopodia and healthy controls.Besides,higher meshing requirements are needed for the calculation of strephenopodia dynamics.Therefore,it was necessary to perform mesh refinement with a size of 1.5 mm for the region of interest (such as the metatarsal bone).The contact area between the plantar soft tissue and the ground was also subjected to mesh refinement with a size of 2 mm.Finally,a total of 1,361,087 mesh cells and 258,620 nodes were obtained.The overall ankle-foot model was placed in the gravity field with a gravity acceleration of 9.8 m/s2.Some scholars have set the foot strike speed to be 5 m/s in some research on calcaneal collision,ankle impact trauma,and falling to the ground[20].In this study,the foot strike speed of the ankle-foot component was set to be 5 m/s,the height of the ankle from the ground was set to be 0.5 mm,the time response was set to be 1.5 ms,and the ground was fixed.Based on this,the possible injury risk caused by the transient concentrated stress at the time of the foot strike was explored under different strephenopodia patterns.The finite element model is shown in Figures 4(b) and (c).

ISSN 2616-5791 Vol.5, Issue 5: 29-40, DOI: 10.25236/AJMHS.2024.050505

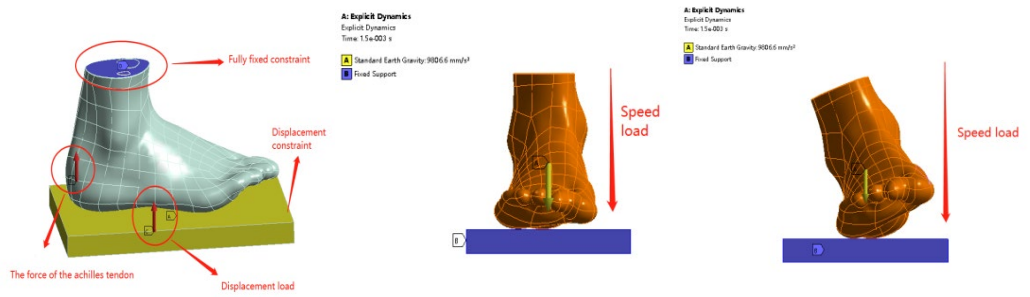

a *b* *c*

Figure 4: Finite element analysis setup.a) Setup of statics boundary conditions.b) Healthy foot.c) Simulated affected foot

2.7. Observation Index

The observation index comprised the stress load distribution from the first to fifth metatarsal bones and tarsometatarsal joints of healthy feet and simulated affected feet under different foot varus angles (0°,10°,15°,and 20°) and under different weight loads.

3. Results

3.1. Statics Finite Element Analysis

(1) The calculation results at the foot varus angles of 0° (healthy),10°,15°,and 20° under 0.5 times the body weight are presented in Figure 5.As the stress nephograms for most bones were similar and there were numerous data points,the calculation results at the foot varus angle of 10° were selected as an example for interpretation.

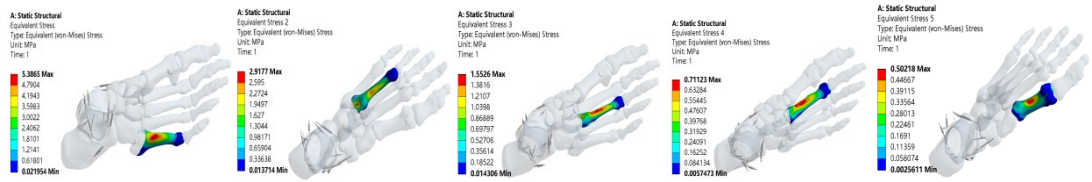

a *b* *c* *d* *e*

Figure 5: Foot strike stress on the metatarsal bone at the foot varus angle of 10° under 0.5 times the body weight.a) Fifth metatarsal bone.b) Fourth metatarsal bone.c) Third metatarsal bone.d) Second metatarsal bone.e) First metatarsal bone

(2) The calculation results of the foot varus angles of 0° (healthy),10°,15°,and 20° under 1 times the body weight are presented in Figure 6.Due to the large number of data points,the calculation results at the foot varus angle of 10° were selected as an example for interpretation.

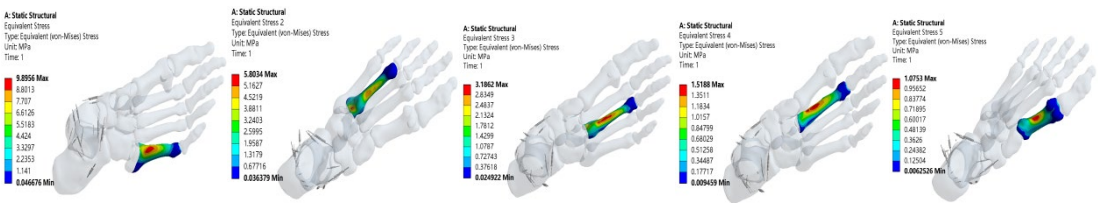

a *b* *c* *d* *e*

Figure 6: Foot strike stress on the metatarsal bone at the foot varus angle of 10° under 1 times thebody weight.a) Fifth metatarsal bone.b) Fourth metatarsal bone.c) Third metatarsal bone.d) Second metatarsal bone.e) First metatarsal bone

ISSN 2616-5791 Vol.5, Issue 5: 29-40, DOI: 10.25236/AJMHS.2024.050505

Table 3: Foot strike stress on the metatarsal bone (MPa) at the foot varus angle of 0° (healthy) under different weight loads

Weight Loads	Fifth Metatarsal Bone	Fourth Metatarsal Bone	Third Metatarsal Bone	Second Metatarsal Bone	First Metatarsal Bone
0.5 times	4.574	4.629	3.280	1.423	0.917
1 times	7.752	8.663	7.053	3.480	2.332
2 times	12.460	15.134	13.639	8.060	6.321

Table 4: Foot strike stress on the metatarsal bone (MPa) at the foot varus angle of 10° under different weight loads

Weight Loads	Fifth Metatarsal Bone	Fourth Metatarsal Bone	Third Metatarsal Bone	Second Metatarsal Bone	First Metatarsal Bone
0.5 times	5.387	2.918	1.553	0.711	0.502
1 times	9.896	5.803	3.186	1.519	1.075
2 times	17.681	11.515	6.650	3.261	2.294

To make the calculation results more intuitive and facilitate further analysis of the data,the control variable method and line diagrams were employed to display and analyze the bone stress under different working conditions,as illustrated in Tables 3-6 and Figures 7-9.

Table 5: Foot strike stress on the metatarsal bone (MPa) at the foot varus angle of 15° under different weight loads

Weight Loads	Fifth Metatarsal Bone	Fourth Metatarsal Bone	Third Metatarsal Bone	Second Metatarsal Bone	First Metatarsal Bone
0.5 times	5.458	2.336	1.291	0.592	0.428
1 times	10.086	4.641	2.625	1.248	0.903
2 times	18.309	9.298	5.382	2.631	1.898

Table 6: Foot strike stress on the metatarsal bone (MPa) at the foot varus angle of 20° under different weight loads

Weight Loads	Fifth Metatarsal Bone	Fourth Metatarsal Bone	Third Metatarsal Bone	Second Metatarsal Bone	First Metatarsal Bone
0.5 times	5.412	2.016	1.110	0.514	0.384
1 times	10.012	3.959	2.220	1.067	0.799
2 times	18.433	7.953	4.532	2.246	1.676

ISSN 2616-5791 Vol.5, Issue 5: 29-40, DOI: 10.25236/AJMHS.2024.050505

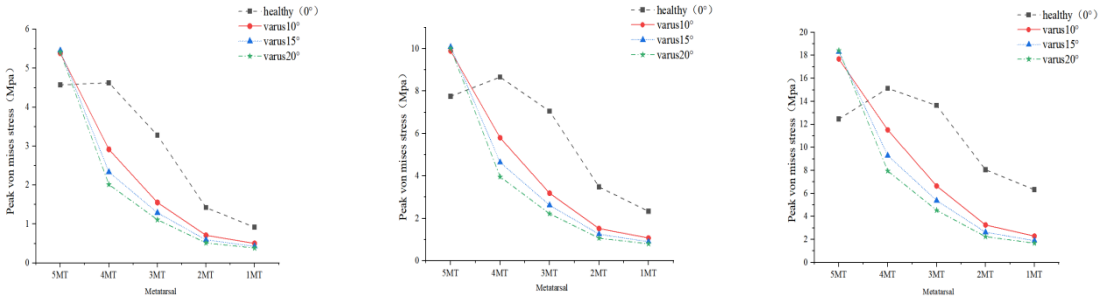

a *b* *c*

Figure 7: Changing trend of the stress on the metatarsal bone under different loads and varus angles.a) 0.5 times the body weight and different varus angles.b) 1 times the body weight and different varus angles.c) 2 times the body weight and different varus angles

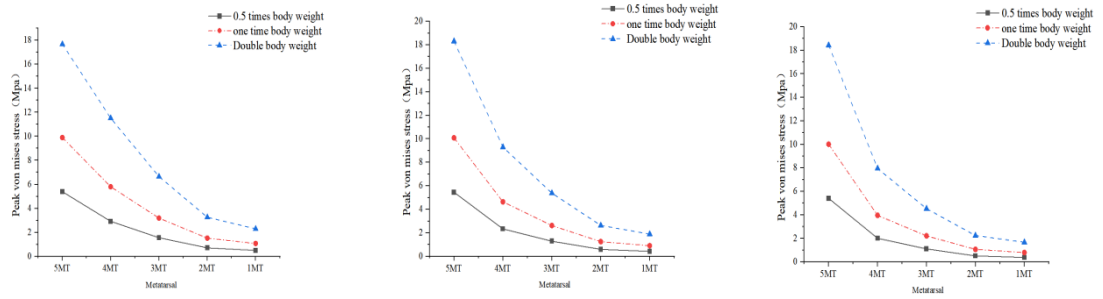

a *b* *c*

Figure 8: Changing trend of the stress on the metatarsal bone under different loads and varus angles.a) At the varus angle of 10° under different loads.b) At the varus angle of 15 °under different loads.c) At the varus angle of 20° under different loads

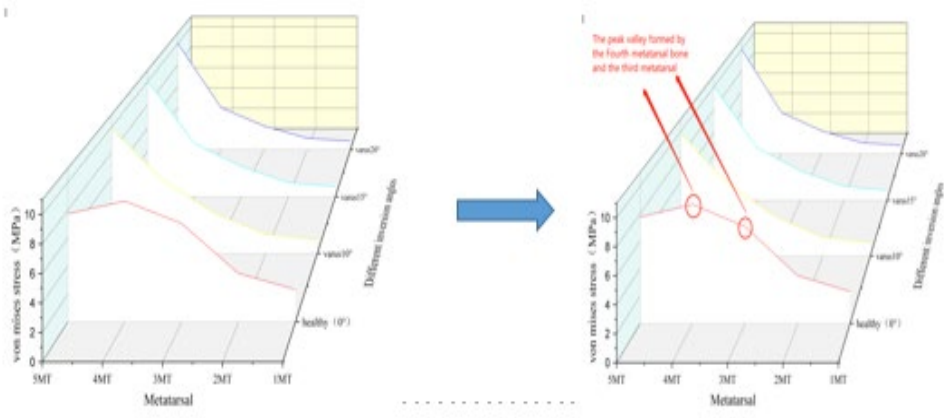

Figure 9: Changing trend of the load on the metatarsal bone of the healthy foot and affected foot under 1 times the body weight

In terms of static data analysis,when the pressure load was constant,as shown in Figure 7 and the tables above,the lateral metatarsal bone was the main weight-bearing component in patients with strephenopodia,while both the lateral and middle parts of the metatarsal bone bore a certain weight in healthy controls.Under 0.5 times the body weight,the stress on the fourth metatarsal bone at the foot varus angles of 10°,15°,and 20° decreased by 36.96%,49.54%,and 56.45%,respectively,compared to healthy controls (0°).Under the same conditions,the stress on the third metatarsal bone decreased by 52.65%,60.64%,and 66.16%,respectively,compared to healthy controls.The stress on these two metatarsal bones gradually decreased with the increase in the foot varus angle,and the decrease ratio also showed an upward trend.This indicated that the larger the varus angle,the less the stress shifted from the fourth metatarsal bone to the third metatarsal bone in the middle part.

The stress load was concentrated and shifted to the lateral fifth metatarsal bone.This finding is consistent with the fact that a larger foot varus angle may increase the risk of stress fractures in the lateral

ISSN 2616-5791 Vol.5, Issue 5: 29-40, DOI: 10.25236/AJMHS.2024.050505

metatarsal bone.Under 1 times the body weight,the stress on the fourth metatarsal bone at the foot varus angles of 10°,15°,and 20° decreased by 33.01%,46.43%,and 54.30%,respectively,compared with healthy controls (0°).Under the same conditions,the stress on the third metatarsal bone decreased by 54.83%,62.78%,and 68.52%,respectively,compared with healthy controls.Notably,the changing trend of stress on these five metatarsal bones in healthy individuals under 1 times the body weight in the simulation study was consistent with the results of WANG et al[21].Under 2 times the body weight,the stress on the fourth metatarsal bone at the foot varus angles of 10°,15°,and 20° decreased by 23.91%,38.56%,and 47.45%,respectively,compared with healthy controls (0°).Under the same conditions,the stress on the third metatarsal bone decreased by 51.24%,60.54%,and 66.77%,respectively,compared with healthy controls.The difference in load on the metatarsal bones under different working conditions can be observed in the fourth and third metatarsal bones.

3.2. Dynamics Finite Element Analysis

The stress distribution trend of bones in the stress nephogram under different foot varus angles was similar to that observed at a foot varus angle of 10° during the foot strike.These stress nephograms will not be listed in this section.The calculated results are presented in Figures 10 and 11,and the stress results for different foot varus angles are listed in Table 7.

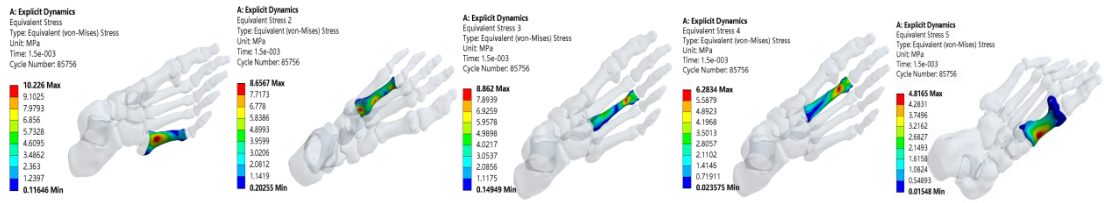

a *b* *c* *d* *e*

a) Fifth metatarsal bone.b) Fourth metatarsal bone.c) Third metatarsal bone. d) Second metatarsal bone.e) First metatarsal bone

Figure 10: Stress on the metatarsal bone of a healthy ankle under the foot strike speed of 5 m/s.

Table 7: Stress on the metatarsal bone (MPa) at different foot varus angles under the foot strike speed of 5 m/s

Location	Healthy Ankle	10°	15°	20°
Fifth Metatarsal Bone	10.226	11.861	12.203	12.043
Fourth Metatarsal Bone	8.657	7.031	6.299	5.924
Third Metatarsal Bone	8.862	4.367	3.587	3.254
Second Metatarsal Bone	6.283	2.220	1.806	1.431
First Metatarsal Bone	4.817	2.332	1.852	1.683

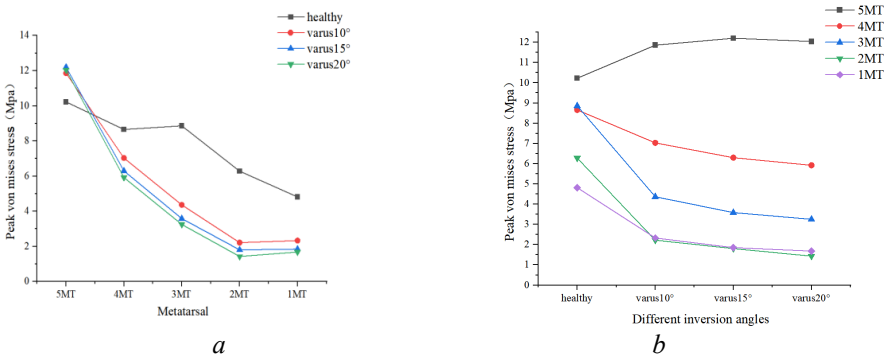

a *b*

Figure 11: Calculation results of stress on bones at the foot strike speed of 5 m/s.a) Changing trend of stress on different bones.b) Comparison of load on the metatarsal bone at different foot varus angles

As shown in Table 7 and Figure 11, this finding was similar to the stress distribution in statics analysis. As the varus angle increased, the stress on the fifth metatarsal bone gradually rose and subsequently stabilized. On the medial side, a notable downward trend was observed from the fourth to the first metatarsal bone. At the time of the foot strike on the ground, the most significant load decrease was

ISSN 2616-5791 Vol.5, Issue 5: 29-40, DOI: 10.25236/AJMHS.2024.050505

observed in the middle third metatarsal bone and the medial second metatarsal bone. The dynamic analysis captured the varying stress trends on the fourth, third, and second metatarsal bones after the foot strike, considering different varus angles at various time points. The results are shown in Figure 12.

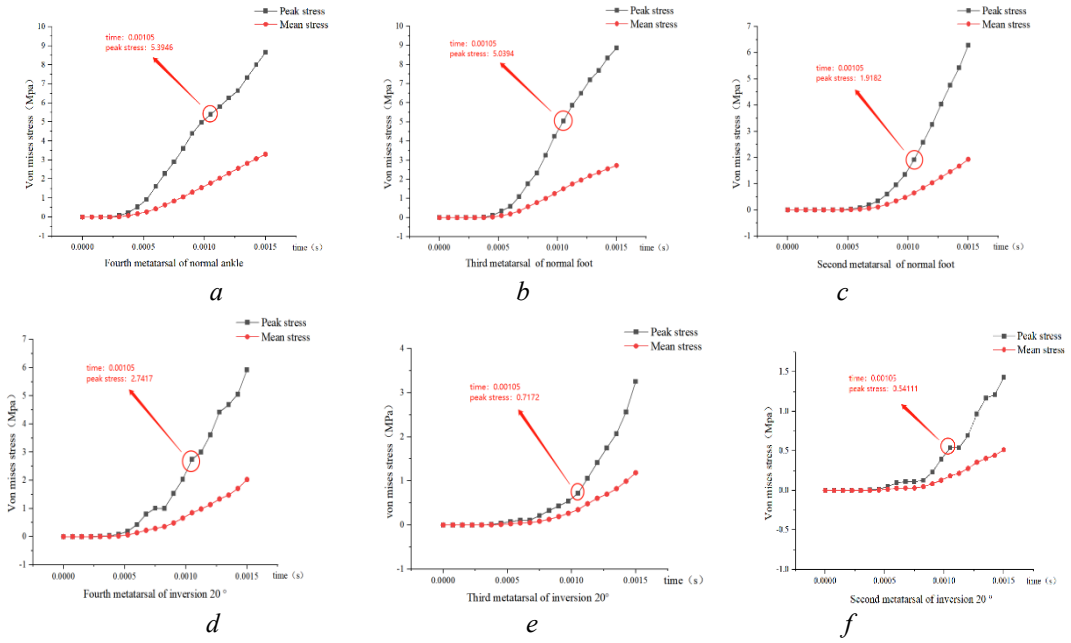

Figure 12: Changing trend of stress on metatarsal bones of the healthy foot and the affected foot (20°) at different time points.a) Stress on the fourth metatarsal bone of the healthy foot.b) Stress on the third metatarsal bone of the healthy foot.c) Stress on the second metatarsal bone of the healthy foot.d) Stress on the fourth metatarsal bone of the affected foot (20°).e) Stress on the third metatarsal bone of the affected foot (20°).f) Stress on the second metatarsal bone of the affected foot (20°)

3.3. Dynamics Finite Element Analysis

As shown in Figures 12(a) and (b),this indicated that the stress on bones increased faster within 1.5 ms after the foot strike.The maximum load on the fourth metatarsal bone of the healthy foot reached 5.395 MPa at a time point close to 1 ms,specifically at 1.05 ms; while the maximum load of the fourth metatarsal bone of the affected foot (20°) was only 2.742 MPa at the same time point.A similar trend was observed in the third and second metatarsal bones as well.The maximum load of the third and second metatarsal bones of the healthy foot was 5.039 MPa and 1.918 MPa,respectively,at the time point of 1.05 ms.In contrast,the maximum load of the third and second metatarsal bones of the affected foot (20°) was only 0.717 MPa and 0.541 MPa,respectively,at the same time point.These data indicate that the foot strike speed and contact area of the middle and medial metatarsal bones of the healthy foot were significantly greater than those of the affected foot within a short time.This may be explained by the fact that the bones on the medial edge of the plantar surface of the affected foot did not come into contact with the ground,or were raised a certain height above it.Additionally,the transfer of stress between bones after the foot strike took longer for the affected foot compared to the healthy foot.

3.4. Contact Area of Soft Tissues and Stress of Tarsometatarsal Joints

The contact area between the lateral side of the foot's soft tissues and the ground is shown in Figures 13(a) and (c).In this study,we compared the data of simulated severe cases (20°) with those of healthy feet.The figures 13(b) and (d) display the comparison results of the lateral tarsometatarsal joints between the two groups.The transient stress on the tarsometatarsal joint of the healthy foot at the time of the foot strike was 66.819 MPa; while that of the affected foot (20°) increased to 95.361 MPa.This suggests that the posterolateral base and tarsometatarsal joint of the fifth metatarsal bone are more susceptible to fractures in patients with strephenopodia.

ISSN 2616-5791 Vol.5, Issue 5: 29-40, DOI: 10.25236/AJMHS.2024.050505

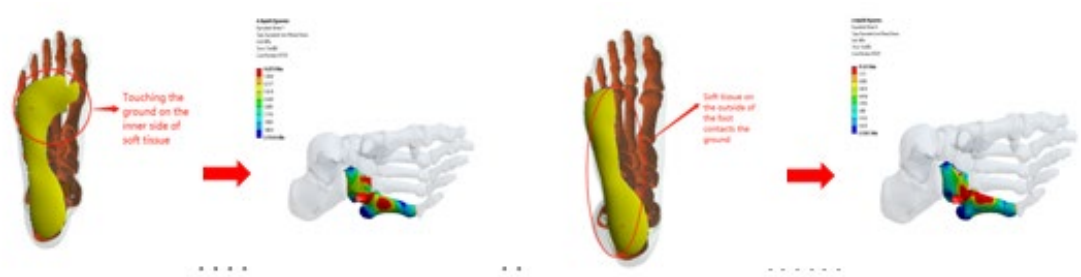

a *b* *c* *d*

Figure 13: Contact area and transient concentrated stress on the lateral tarsometatarsal joint of the healthy foot and the affected foot (20°).a) Contact area of the healthy foot.b) Stress on the tarsometatarsal joint of the healthy foot.c) Contact area of the affected foot.d) Stress on the tarsometatarsal joint of the affected foot (20°)

4. Discussion

In this study,the finite element method was employed to simulate the load changes on the metatarsal bones of healthy and affected feet,both in a static standing state and after a foot strike at a specific speed during walking.The comprehensive analysis revealed a significant difference in metatarsal loads between healthy and affected feet,specifically in the fourth,third,and second metatarsal bones,following a foot strike.The stress on the fifth metatarsal bone of the affected foot increased significantly,with the lateral aspect of this bone having the highest risk of suffering from stress fractures.Additionally,the bone load points of healthy and affected feet were analyzed under varying conditions,specifically after a foot strike.During rehabilitation,it is necessary to correct the calcaneus and the first metatarsal bone.Furthermore,raising the fifth metatarsal bone is required to achieve ankle joint eversion.

In addition,the bone stress curves were observed at different varus angles.It was found that as the varus angle increased from 10° to 20°,the load transfer from the fifth metatarsal bone to the fourth metatarsal bone decreased sharply.The stress curves changed significantly in these two regions,and this trend exhibited similar patterns under different body weights.For example,when considering a load of 1 times the body weight,the stress transfer decreased by 41.36%,53.99%,and 60.46% under varus angles of 10°,15°,and 20°,respectively.These data indicated that,with a constant load,as the varus angle increased,the load on the fourth metatarsal bone decreased.Moreover,the decrease ratio also became larger with a greater varus angle.This further verified that patients with strephenopodia had higher risks of stress fractures in the fifth metatarsal bone compared with healthy individuals[22].

The stress on the fifth metatarsal bone would increase with the increase of the varus angle.However,the lateral soft tissue of the affected foot was only loaded by the fifth metatarsal bone,and there would be less stress transmitted to other bones.As a result,these lateral metatarsal bones had basically the same load under different varus angles.This can be attributed to the small contact between the medial edge of soft tissues and the ground.This would further induce a larger load on the fifth metatarsal base and the lateral tarsometatarsal joint of the foot compared with the healthy foot.

In the clinical treatment of foot deformities,it is difficult for orthopedists and clinicians to define the correction site in the affected foot.They often implement the treatment based on personal experience and skills.Mild foot deformities in daily life are often ignored by patients.Moreover,the hazards of foot deformities have not been fully recognized by patients and their families.The persistent existence of this condition may lead to foot bone injury,stress fracture,and other risks.In this study,the hazards of foot deformities and the adverse effects of larger varus angles were clarified through a comparative analysis between affected and healthy feet.These findings may provide valuable reference for the correction of foot deformities in subsequent clinical practice.

5. Conclusion

In this study,the effects of various pathological parameters,including foot varus angles of 0°,10°,15°,and 20° and weight loads ranging from 0.5 to 2 times the body weight,on the local bone loading of feet were analyzed using the finite element numerical simulation method.Furthermore,the mechanical changes in each metatarsal bone of the affected foot were investigated from various perspectives.Additionally,by comparing the data,the primary difference in weight-bearing metatarsal

ISSN 2616-5791 Vol.5, Issue 5: 29-40, DOI: 10.25236/AJMHS.2024.050505

points under a static standing state between healthy and affected feet was identified.It was found that a smaller varus angle was conducive to a reduced risk of high loads on the lateral tarsometatarsal joint and stress fractures of the fifth metatarsal bone.As the foot varus angle increased,the stress transfer between the metatarsal bones of the affected foot during foot strike took longer than that of the healthy foot.This resulted in a smaller load on the fourth to the first metatarsal bone in the medial part of the affected foot compared to the healthy foot.Furthermore,the transient foot strike speed and the area of contact for the metatarsal bones in the middle and medial parts of the healthy foot were significantly greater than those of the affected foot.This may contribute to the difference in the loading on the fourth and third metatarsal bones between healthy and affected feet,these findings may lay a solid foundation for clinical rehabilitation of strephenopodia from the perspective of reducing the load on different metatarsal bones.

Conflict of Interest

The authors claim that there are no potential conflicts of interest in the research, authorship, and/or publication of this article.

Acknowledgements

Basic Scientific Research Fund Project of Universities Directly under the Inner Mongolia Autonomous Region in 2022, No. JY20220026 (to WK); Scientific Research Start-Up Fund Project of Inner Mongolia University of Technology in 2021, (to WK)

References

[1] National Research Center for Rehabilitation Technical Aids.Principle and Practice for Foot Correction.Beijing: China Social Publishing House.2009
[2] Yu HX.Observation of the therapeutic effect of correcting foot varus on improving knee hyperextension and gait in patients after stroke.Current neurovascular research.18(3),pp. 314-317,2021.
[3] Ward AB.A literature review of the pathophysiology and onset of post-stroke spasticity.European journal of neurology.19(1),pp.321-27,2012.
[4] Zhang LL,Wang MS,Xu DW,Huang H,Yang YT.Three-dimensional finite element modeling of the foot and its multi-posture biomechanical analysis.Chinese Journal of Tissue Engineering Research. 25(30), pp. 4799-4804,2021.
[5] Li SD,Gu YD.A finite element study of the stress on metatarsals during forefoot strike at different angles.Sports Science.38(3),pp.67-72+97,2018.
[6] He XY,Wang CQ,Zhou ZP,Zhang ZN,Lai CS,Ruan KM,Li XL,Zhao DW.Establishment of normal foot and common foot disease models using three-dimensional finite element method and biomechanical analysis.Chinese Journal of Tissue Engineering Research.24(9),pp.1410-1415,2020.
[7] Kathirgamanathan B,Silva P,Fernandez J.Implication of obesity on motion,posture and internal stress of the foot: an experimental and finite element analysis.Computer methods in biomechanics and biomedical engineering.22(1),pp.47-54,2018.
[8] Zhang HW,Chen L,Yang JY,Liu Y,Zheng YJ.Biomechanical study of heel pain during push-off period based on finite element method.Chinese Journal of Biomedical Engineering.39(2),pp.190-196,2020.
[9] Liu XY,Yue Y,Wu XY,Huang XW,Hao YH,Lu Y.Analysis of transient response of the human foot based on the finite element method.Technology and health care: official journal of the European Society for Engineering and Medicine.30(1),pp.79-92,2021.
[10] Gu YD,Ren XJ,Li JS,Lake MJ,Zhang QY,Zeng YJ.Computer simulation of stress distribution in the metatarsals at different inversion landing angles using the finite element method.International orthopaedics.34(5),pp.669-676,2010.
[11] Zhang QQ.Finite element analysis of three-dimensional composite model of foot and its application.Ph.D.Thesis,Hefei University of Technology.2014.
[12] Jin QK.Construction and verification of three-dimensional finite element simulation model of human foot and ankle.Ph.D.Thesis,Dalian Medical University.2015.
[13] Cho JR,Lee DY,Ahn YJ.Finite element investigation of the biomechanical responses of human foot to the heel height and a rigid hemisphere cleat. Journal of Mechanical Science and Technology. 30(9),pp. 4269-4274, 2016.
[14] Liu QH. Establishment and analysis on digital three-dimensional finite element model of human foot and ankle.Ph.D.Thesis,Southern Medical University.2010.

ISSN 2616-5791 Vol.5, Issue 5: 29-40, DOI: 10.25236/AJMHS.2024.050505

[15] Darwich A,Nazha H,Nazha A,Daoud M,Alhussein A.Bio-Numerical Analysis of the Human Ankle-Foot Model Corresponding to Neutral Standing Condition.Journal of biomedical physics & engineering. 10(5), pp.645-650,2020.
[16] Wang D,Cai P.Finite Element Analysis of the Expression of Plantar Pressure Distribution in the Injury of the Lateral Ligament of the Ankle.Nano Biomedicine and Engineering.11(5),pp.290-296,2019.
[17] Gong TS,Kang LP,Li S,Guo SY,Zhang SY,Du MX.Finite element analysis of foot model and its verification.China Leather.51(4),pp.61-66,2023.
[18] Fan YB,Wang LZ.Biomechanical modeling and simulation on musculoskeletal system.Beijing: People's Medical Publishing House.2018.
[19] Cheung JT,Zhang M,An KN.Effect of Achilles tendon loading on plantar fascia tension in the standing foot.Clinical biomechanics (Bristol,Avon).21(2),pp.194-203,2006.
[20] Wong WC,Niu WX,Wang Y,Zhang M.Finite Element Analysis of Foot and Ankle Impact Injury: Risk Evaluation of Calcaneus and Talus Fracture.PloS one.11(4),pp.e0154435,2016.
[21] Wang CQ,He XY,Zhang ZN,Lai CS,Li XL,Zhou ZP,Ruan KM.Three-Dimensional Finite Element Analysis and Biomechanical Analysis of Midfoot von Mises Stress Levels in Flatfoot,Clubfoot,and Lisfranc Joint Injury.Med Sci Monit.27(4),pp.e931969,2021.
[22] Riegger M,Mueller J,Giampietro A,Saporito A,Filardo G,Treglia G,Guidi M,Candrian C.Forefoot Adduction,Hindfoot Varus or Pes Cavus: Risk Factors for Fifth Metatarsal Fractures and Jones Fractures? A Systematic Review and Meta-Analysis.The Journal of foot and ankle surgery: official publication of the American College of Foot and Ankle Surgeons. 61 (3), pp. 641-647,2022.